

## Ferromagnetic ordering and weak spin-glass-like effect in $\text{Pr}_2\text{CuSi}_3$ and $\text{Nd}_2\text{CuSi}_3$

This article has been downloaded from IOPscience. Please scroll down to see the full text article.

2009 J. Phys.: Condens. Matter 21 026006

(<http://iopscience.iop.org/0953-8984/21/2/026006>)

View [the table of contents for this issue](#), or go to the [journal homepage](#) for more

Download details:

IP Address: 129.252.86.83

The article was downloaded on 29/05/2010 at 17:04

Please note that [terms and conditions apply](#).

# Ferromagnetic ordering and weak spin-glass-like effect in $\text{Pr}_2\text{CuSi}_3$ and $\text{Nd}_2\text{CuSi}_3$

Dexin Li<sup>1</sup>, Xiang Zhao<sup>1</sup> and Shigeki Nimori<sup>2</sup>

<sup>1</sup> Key Laboratory for Anisotropy and Texture of Materials (Ministry of Education), Northeastern University, Shenyang 110004, People's Republic of China

<sup>2</sup> Tsukuba Magnet Laboratory, National Institute for Materials Science, 3-13 Sakura, Tsukuba 305-0003, Japan

E-mail: [dxli@imr.tohoku.ac.jp](mailto:dxli@imr.tohoku.ac.jp)

Received 17 June 2008, in final form 22 October 2008

Published 9 December 2008

Online at [stacks.iop.org/JPhysCM/21/026006](http://stacks.iop.org/JPhysCM/21/026006)

## Abstract

We present the results of the temperature dependences of ac and dc susceptibilities, high-field magnetization, magnetic relaxation, specific heat, and electrical resistivity of  $\text{Pr}_2\text{CuSi}_3$  and  $\text{Nd}_2\text{CuSi}_3$ , compounds previously shown in the literature to exhibit interesting properties. It is observed that the investigated compounds undergo a ferromagnetic phase transition at a characteristic temperature  $T_C$  ( $= 9.8$  K for  $\text{Pr}_2\text{CuSi}_3$  and  $5.6$  K for  $\text{Nd}_2\text{CuSi}_3$ ), where zero-field-cooled dc susceptibility shows a rapid increase followed by a sharp peak just below  $T_C$ . Below  $T_C$ , the magnetization curve displays an open hysteresis loop and a steep rise at low fields, while irreversible magnetism and long-time magnetic relaxation effects can be observed. Furthermore, near  $T_C$  both the real and imaginary components of the ac susceptibility show a large peak with a small frequency shift of the peak position, and a sharp anomaly appears in the specific heat and electrical resistivity curves. These unusual features observed for  $\text{Pr}_2\text{CuSi}_3$  and  $\text{Nd}_2\text{CuSi}_3$  strongly suggest the formation of huge ferromagnetic clusters accompanied by a very weak spin-glass-like effect in both samples. The obtained results are discussed by comparing them with the data reported for other 2:1:3 intermetallic compounds and some alloyed compounds with different stoichiometry.

## 1. Introduction

Ternary intermetallic compounds with general formula  $\text{R}_2\text{MX}_3$  ( $\text{R} = \text{rare earth or U}$ ,  $\text{M} = \text{transition metals}$ ,  $\text{X} = \text{Si, Ge, Ga, In}$ ) have become the subjects of intensive studies during the last decade. Many members of the  $\text{R}_2\text{MX}_3$  compounds have  $\text{AlB}_2$ - or  $\text{CaIn}_2$ -type crystal structures, which consist of  $\text{R}$  and  $\text{M-X}$  layers alternating along the  $c$ -axis, and possible crystallographic disorder within  $\text{M-X}$  positions. Various magnetic ground states with complicated magnetic structures originating from such distinctive crystal structures have been found for  $\text{R}_2\text{MX}_3$  systems in recent years. The typical examples are the uranium-based compounds  $\text{U}_2\text{MSi}_3$ , which show numerous unusual magnetic properties strongly related to the crystal structure of the sample. Compounds  $\text{U}_2\text{MSi}_3$  with  $\text{M} = \text{Pd, Pt, Au, Ir}$  and  $\text{Rh}$  are found to show spin glass (SG) or cluster glass behavior below their respective

spin freezing temperature  $T_f$  [1–5]. The crystal structures of these compounds are confirmed to be the derived  $\text{AlB}_2$ -types with completely or partially disordered  $\text{M}$  and  $\text{Si}$  atoms at  $\text{B}$  crystallographic sites. In contrast, for  $\text{U}_2\text{MSi}_3$  with  $\text{M} = \text{Fe, Ru, and Os}$ , which crystallize in the  $\text{U}_2\text{RuSi}_3$ -type structure with a perfectly ordered arrangement of  $\text{M}$  and  $\text{Si}$  atoms, no SG behavior can be observed [2, 3, 6, 7]. On the other hand, interesting magnetic properties were also observed in rare-earth 2:1:3 compounds, such as typical SG behavior in  $\text{Ce}_2\text{NiGe}_3$  [8],  $\text{Ce}_2\text{CuGe}_3$  [9],  $\text{Ce}_2\text{AgIn}_3$  [10] and  $\text{Nd}_2\text{AgIn}_3$  [11], ferromagnetic order in  $\text{Nd}_2\text{MSi}_3$  ( $\text{M} = \text{Rh, Pd, Pt}$ ) [12–14], antiferromagnetic order in  $\text{Tb}_2\text{AgIn}_3$  [15] and  $\text{R}_2\text{CuIn}_3$  ( $\text{R} = \text{Nd, Dy, Ho}$ ) [16], and coexistence of SG state and long-range magnetic order in  $\text{Dy}_2\text{PdSi}_3$ ,  $\text{Tb}_2\text{PdSi}_3$ , and  $\text{Tb}_2\text{CuIn}_3$  [17–20] etc. In general, it is accepted that the SG state in some  $\text{R}_2\text{MX}_3$  compounds originates from the random arrangement of the nonmagnetic atoms, and thus these systems

are usually called nonmagnetic atom disorder (NMAD) spin glasses.

Rare-earth copper silicides  $R_2CuSi_3$  ( $R$  = rare earth elements) form another family in ternary 2:1:3 intermetallic compounds. In this family, apart from  $Ce_2CuSi_3$  [21] and  $Eu_2CuSi_3$  [22] which were found to show cluster glass and ferromagnetic behavior below the spin freezing temperature  $T_f = 2.7$  K and the Curie temperature  $T_C = 37$  K, respectively, research work on physical properties was reported only for  $Pr_2CuSi_3$  in 1997 [23] and for  $Nd_2CuSi_3$  in 1998 [24] by Tien *et al*. The former was classified as an SG material exhibiting ferromagnetism at  $T_C = 10$  K, and the latter was considered to have an antiferromagnetic transition at  $T_N = 5$  K and SG properties below 5 K. For both  $Pr_2CuSi_3$  and  $Nd_2CuSi_3$ , irreversible magnetism manifesting itself as the difference between the field cooling (FC) and zero-field cooling (ZFC) magnetization was observed below  $T_C/T_N$  in a low field, and larger specific heat coefficients ( $\gamma$ ) of the  $T$ -linear term were estimated from the specific heat measurements. On the other hand, based on the x-ray diffraction patterns,  $Pr_2CuSi_3$  and  $Nd_2CuSi_3$  were considered to crystallize in the hexagonal  $AlB_2$ -type structure with strong site disorder among Cu and Si atoms. Thus compound  $Pr_2CuSi_3$  was classified as an NMAD spin glass [23].

Very recently the electron diffraction observation performed by Yubuta *et al* [25] clearly indicates the existence of Cu–Si superstructure in our  $Pr_2CuSi_3$  and  $Nd_2CuSi_3$  samples (similar to that reported for  $U_2IrSi_3$  [26]) suggesting the ordered distribution of Cu and Si atoms, although it could not be confirmed within the limit of the x-ray diffraction technique. In this sense, the SG behavior reported to exist in these compounds is extraordinary and interesting in physics, because it is hard to understand the presence of randomness and frustration (the necessary conditions to form the SG state) in a compound with ordered crystal structure [27]. Moreover, irreversible magnetism is not always the sign of SG behavior, it is also a common feature for magnetic materials with long-range magnetic order [28]. These motivate us to carry out detailed magnetic property measurements on the two compounds, including the temperature dependence of ac susceptibility at various frequencies that could offer a good criterion for distinguishing a canonical SG from an SG-like material. In this paper we will mainly present the experimental results, and discuss the observed anomalous magnetic behaviors by comparing our data with those obtained for other 2:1:3 systems and some alloyed compounds with different stoichiometry.

## 2. Experimental details

Polycrystalline samples of about 3.5 g for  $Pr_2CuSi_3$  and about 4 g for  $Nd_2CuSi_3$  were prepared by melting high-purity starting elements in a four-electrode arc furnace. The buttons were flipped and remelted several times to ensure homogeneity, and then annealed at high temperature ( $500^\circ\text{C} \times 168$  h +  $750^\circ\text{C} \times 168$  h for  $Pr_2CuSi_3$ ,  $950^\circ\text{C} \times 480$  h for  $Nd_2CuSi_3$ ) in evacuated sealed quartz tubes. Both x-ray powder diffraction measurement and electron diffraction observation are used to check the sample's quality and

examine the crystal structure. The samples used for x-ray powder diffraction, electron diffraction, and magnetic measurements are cut from the same annealed button. The ac susceptibility  $\chi_{ac}(T)$ , dc magnetization  $M(T)$ , and magnetic relaxation  $M(t)$  measurements were performed in a Quantum Design superconducting quantum interference device (SQUID) magnetometer. Using a hybrid magnet, the high-field magnetization was measured at 4.2 K by means of a sample extraction method up to 280 kOe, and the absolute value of the magnetization was calibrated using the data measured by a SQUID. The adiabatic heat pulse method and a standard four-terminal dc method were employed for specific heat  $C(T)$  and electrical resistivity  $\rho(T)$  measurements, respectively.

## 3. Experimental results and analysis

The x-ray powder diffraction measurements of the  $Pr_2CuSi_3$  and  $Nd_2CuSi_3$  samples were performed at room temperature with  $Cu\ K\alpha$  radiation. Although the diffraction lines can be indexed based on the disordered hexagonal  $AlB_2$ -type structure model (space group  $P6/mmm$ ) with Pr/Nd atoms on 1a sites and Cu and Si atoms statistically distributed over the 2d sites, the electron diffraction patterns and the high-resolution image obtained by Yubuta *et al* prove clear evidence for the presence of a Cu–Si superstructure in both the  $Pr_2CuSi_3$  and  $Nd_2CuSi_3$  samples suggesting the ordered arrangement of Cu and Si atoms (the detailed experimental and analytical results will be published elsewhere) [25]. Similar superstructure had been confirmed to exist in the compound  $U_2IrSi_3$  [26]. In fact, powder x-ray diffraction measurements, in many cases, cannot find the existence of superlattices due to the limit of the x-ray technique. Based on these results, it seems to be more reasonable to consider the  $Pr_2CuSi_3$  and  $Nd_2CuSi_3$  samples as crystallographic ordered compounds (with the structure derived from the hexagonal  $AlB_2$ -type) than NMAD systems. With this structural image in mind we show the magnetic property measurements of our  $Pr_2CuSi_3$  and  $Nd_2CuSi_3$  samples and discuss the experimental results in the following.

The temperature dependences of dc magnetization  $M(T)$  of  $Pr_2CuSi_3$  and  $Nd_2CuSi_3$  were measured in the FC mode and in the ZFC mode between 1.8 and 300 K. Figures 1(a) and (b) show the ZFC data in a field of  $H = 100$  Oe plotted as  $M(T)/H$  versus  $T$  (hereafter, we call  $M(T)/H$  dc susceptibility and note it as  $\chi(T)$ ). At high temperatures, the observed  $\chi_{ZFC}(T)$  behavior can be fitted using the Curie–Weiss law with the values of the Curie–Weiss temperature  $\theta_p = 7.5$  and 5.9 K and the effective magnetic moment  $\mu_{eff} = 3.59 \mu_B/Pr$  and  $3.68 \mu_B/Nd$  for  $Pr_2CuSi_3$  and  $Nd_2CuSi_3$ , respectively (see the insets of figures 1(a) and (b)). At low temperatures, a large and sharp peak is observed at  $T_m$  just below the temperature ( $T_C = 9.8$  and 5.6 K for  $Pr_2CuSi_3$  and  $Nd_2CuSi_3$ , respectively) where  $d\chi_{ZFC}(T)/dT$  shows the largest value, indicating some kind of magnetic phase transition near this temperature. In this paper,  $T_C$  is defined as the magnetic phase transition temperature. The temperature dependences of specific heat and electrical resistivity of  $Pr_2CuSi_3$  and  $Nd_2CuSi_3$  are illustrated in figures 1(c)–(f). The

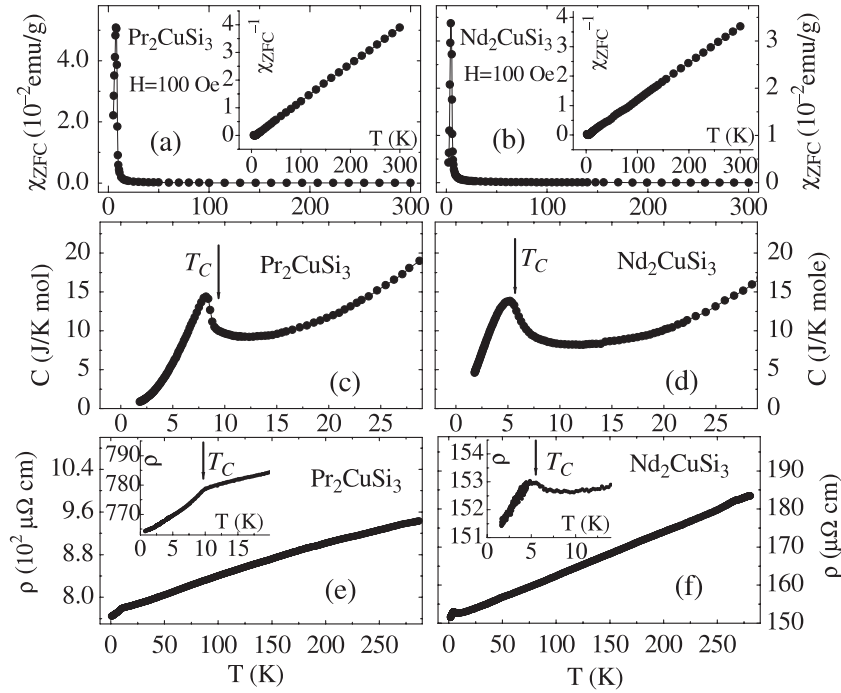


**Figure 1.** Temperature dependences of dc susceptibility ((a), (b)), specific heat ((c), (d)), and electrical resistivity ((e), (f)) of  $\text{Pr}_2\text{CuSi}_3$  and  $\text{Nd}_2\text{CuSi}_3$ . The insets of (a) and (b) show the Curie–Weiss behaviors of the reciprocal dc susceptibility of  $\text{Pr}_2\text{CuSi}_3$  and  $\text{Nd}_2\text{CuSi}_3$ , respectively. The insets in (e) and (f) highlight the electrical resistivity around magnetic phase transition temperature for  $\text{Pr}_2\text{CuSi}_3$  and  $\text{Nd}_2\text{CuSi}_3$ , respectively. The units of  $\chi_{\text{ZFC}}^{-1}$  and  $\rho$  in the insets of (a), (b) and (e), (f) are  $10^4 \text{ g emu}^{-1}$  and  $\mu\Omega \text{ cm}^{-1}$ , respectively.

important observations are that a large peak in  $C(T)$  and an evident kink in the  $\rho(T)$  curves appear at the temperature ( $T_{\text{sf}}$  and  $T_{\rho}$ , respectively) near  $T_C$  for both samples, suggesting the existence of long-range magnetic ordering below  $T_C$ , in agreement with the susceptibility measurements (figures 1(a) and (b)).

Tien *et al* had reported similar properties, with a detailed discussion on the specific heat and electrical resistivity behaviors [23, 24]. In the literature, magnetic specific heat of  $\text{R}_2\text{CuSi}_3$  ( $\text{R} = \text{Pr}$  and  $\text{Nd}$ ) was defined as  $C_{\text{m}}(T) = C(\text{R}_2\text{CuSi}_3) - C(\text{La}_2\text{CuSi}_3)$ , and the large  $\gamma$  values of  $505 \text{ mJ mol}^{-1} \text{ K}^{-2}$  for  $\text{Pr}_2\text{CuSi}_3$  and  $753 \text{ mJ mol}^{-1} \text{ K}^{-2}$  for  $\text{Nd}_2\text{CuSi}_3$  were determined from the  $C_{\text{m}}/T-T^2$  plots using the data between 20 and 40 K. For  $\text{Pr}_2\text{CuSi}_3$ , we have performed a similar analysis using our specific heat data between 2 and 4 K, and obtained the  $\gamma$  value to be  $342 \text{ mJ mol}^{-1} \text{ K}^{-2}$  ( $171 \text{ mJ (mol-Pr)}^{-1} \text{ K}^{-2}$ ). Since specific heat  $C(T) = C_{\text{p}}(T) + C_{\text{e}}(T) + C_{\text{m}}(T)$  contains contributions from vibrational ( $C_{\text{p}}$ ), electronic ( $C_{\text{e}}$ ), and magnetic ( $C_{\text{m}}$ ) parts, based on our experimental data it is impossible to accurately separate the electronic part and magnetic part. Firstly, the temperatures of our measurements are not low enough relative to  $T_C$ , thus the magnetic contribution (including the possible influence of low-lying crystal levels and/or SG-like effect) should enhance the  $\gamma$  value. Secondly, considering that the large  $\gamma$  values have been determined for many 2:1:3 f-electronic systems even for  $\text{U}_2\text{RuSi}_3$ , the paramagnetic compound with ordered arrangement of all atoms and no SG behavior [4], we cannot rule out the contribution from the heavy fermion mechanism, although no evident heavy fermion

behavior was found in  $\rho(T)$  measurements [23]. These mechanisms are also applicable for  $\text{Nd}_2\text{CuSi}_3$ , although our  $C(T)$  data below  $T_C$  cannot be used to estimate the  $\gamma$  value due to its much lower magnetic transition temperature.

In figure 2 we compare the FC and ZFC susceptibilities measured in different magnetic fields for the  $\text{Pr}_2\text{CuSi}_3$  and  $\text{Nd}_2\text{CuSi}_3$  samples. It is clear from this figure that there is no difference between the FC and ZFC curves in the paramagnetic state, and the magnetic transition peak can be observed only in the  $\chi_{\text{ZFC}}(T)$  curve at a strongly field dependent temperature  $T_{\text{m}}(H)$ . Moreover, irreversible magnetism manifesting itself as the bifurcation between the  $\chi_{\text{FC}}(T)$  and  $\chi_{\text{ZFC}}(T)$  curves appears at low temperatures. With increasing  $H$ , the peak in  $\chi_{\text{ZFC}}(T)$  becomes broader and its height decreases, the peak temperature  $T_{\text{m}}$  shifts toward lower temperatures, while almost no change can be observed for  $T_C$ . This irreversible magnetism indicates the metastable feature of the ground state of  $\text{Pr}_2\text{CuSi}_3$  and  $\text{Nd}_2\text{CuSi}_3$ , and is similar to the character usually observed in some magnetic materials with long-range magnetic order or in SG systems. Above 2 kOe,  $\chi_{\text{FC}}(T)$  and  $\chi_{\text{ZFC}}(T)$  coincide with each other, and no peak can be observed even in the  $\chi_{\text{ZFC}}(T)$  curve for either sample.

The distinction between FC and ZFC dc susceptibilities described above indicates the nonequilibrium character of the low-temperature magnetic states in  $\text{Pr}_2\text{CuSi}_3$  and  $\text{Nd}_2\text{CuSi}_3$ . Thermodynamically, such nonequilibrium states directly relate to slow dynamics. In figure 3, we present the magnetic relaxation behavior of  $\text{Pr}_2\text{CuSi}_3$  and  $\text{Nd}_2\text{CuSi}_3$  in magnetic field  $H = 500$  and 0 Oe by plotting the data of  $M(t)/M(0)$  as a function of time  $t$ . The sample was first cooled in zero field

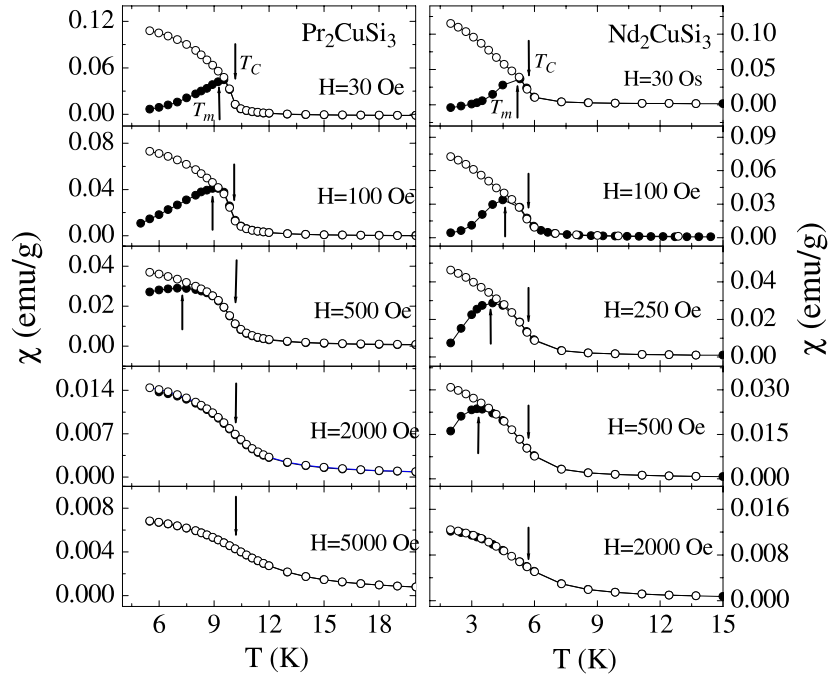


**Figure 2.** Temperature dependences of field-cooled (O) and zero-field-cooled (●) dc susceptibility ( $\chi = M/H$ ) of  $\text{Pr}_2\text{CuSi}_3$  and  $\text{Nd}_2\text{CuSi}_3$  in various applied fields. The down arrows indicate the temperatures where  $\chi$  shows the maximum temperature rate of change, the upward arrows indicate the peak temperatures in  $\chi_{\text{ZFC}}(T)$  curves.

from a temperature far above  $T_C$  to the desired temperature. Then a field of 500 Oe was applied and  $M(t)$  was measured in this field for about 2 h for  $\text{Pr}_2\text{CuSi}_3$  (figure 3(a)) and about 1 h for  $\text{Nd}_2\text{CuSi}_3$  (figure 3(b)). Next, the magnetic field was switched off and  $M(t)$  was recorded again in zero field (see the insets of figure 3). For  $\text{Pr}_2\text{CuSi}_3$  the decay of  $M(t)$  is remarkably slow, nonsaturation magnetization in 500 Oe and nonzero remanence in zero field can be observed even after waiting for 2 h. Similar long-time magnetic relaxation behavior is also evident for  $\text{Nd}_2\text{CuSi}_3$ , as illustrated in figure 3(b). Using a logarithmic function,  $M(t) = M_0 - S \ln(t + t_0)$ , the obtained relaxation behaviors shown in figure 3 can be fitted very well over the full time range studied with three  $H$ - and  $T$ -dependent fitting parameters: initial zero-field magnetization  $M_0$ , magnetic viscosity  $S$ , and characteristic time  $t_0$ . The best fitting results obtained by using the least-squares method are shown by the solid lines in figure 3 with positive and negative  $S$  values in zero field and 500 Oe, respectively.

It is interesting to note that the characteristic phenomenon of irreversible magnetism and magnetic relaxation on a macroscopic timescale can be observed for ferromagnets with high magnetic anisotropy [29] below their Curie temperatures and for all spin glasses below their spin freezing temperatures [27–30]. Also, the logarithmic function could be used to reproduce the time dependence of magnetization for either the SG system or the ferromagnetic material subject to hysteresis. In order to explore the possible SG effect, we have performed ac susceptibility measurements in the frequency range  $0.1 \text{ Hz} \leq \omega/2\pi \leq 1000 \text{ Hz}$  on the  $\text{Pr}_2\text{CuSi}_3$  and  $\text{Nd}_2\text{CuSi}_3$  samples. The data of the real component,  $\chi'_{\text{ac}}(T)$ , of the ac susceptibility are illustrated in figure 4. A

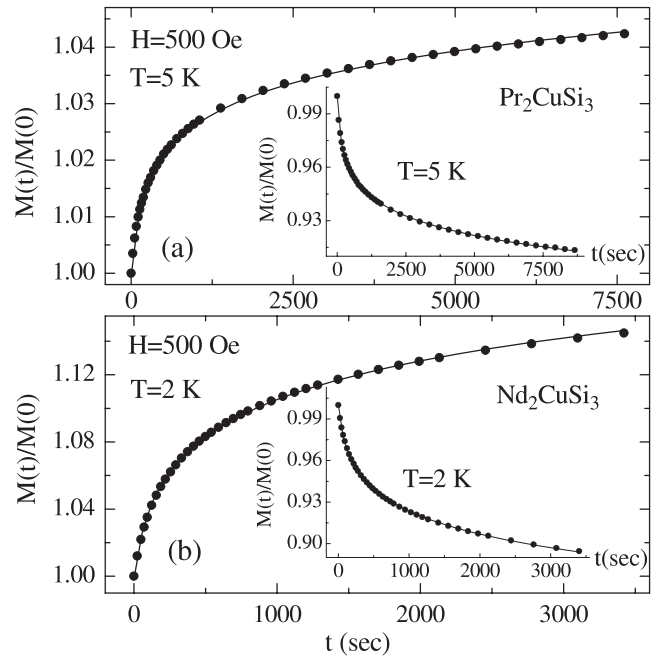


**Figure 3.** Magnetic relaxation behavior measured in an applied field of 500 Oe at 5 K for  $\text{Pr}_2\text{CuSi}_3$  (a) and at 2 K for  $\text{Nd}_2\text{CuSi}_3$  (b), plotted as  $M(t)/M(0)$  versus  $t$ . The insets in (a) and (b) display the time dependence of the remanent magnetization at 5 and 2 K for  $\text{Pr}_2\text{CuSi}_3$  and  $\text{Nd}_2\text{CuSi}_3$ , respectively. The solid lines represent least-squares fits using the equation.

pronounced maximum is observed in the  $\chi'_{\text{ac}}(T)$  curve around a characteristic temperature  $T_{\text{ac}}(\omega)$  for both samples. The  $T_{\text{ac}}$  value is determined to be 9.79 and 5.57 K at  $\omega/2\pi =$

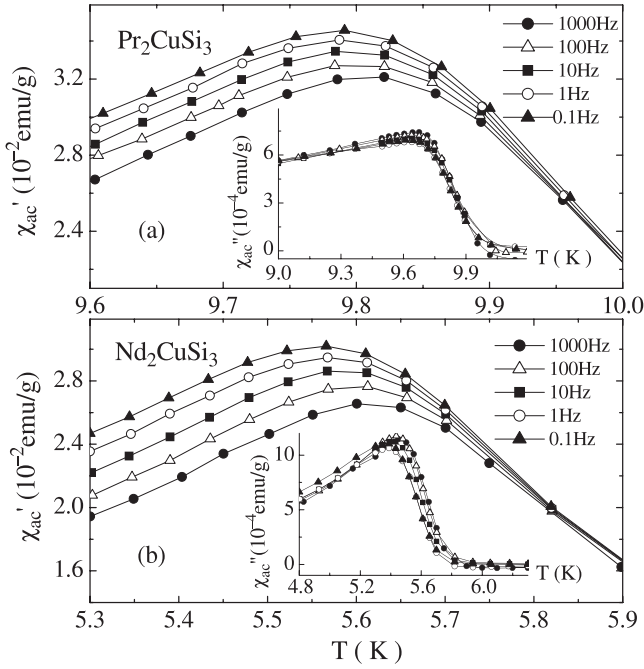


**Figure 4.** Temperature dependences of real and imaginary (inset) components of the ac susceptibility for  $\text{Pr}_2\text{CuSi}_3$  (a) and  $\text{Nd}_2\text{CuSi}_3$  (b) at various frequencies.

0.1 Hz (in good agreement with the  $T_C$  values shown in figure 2), which shifts to 9.82 and 5.61 K at  $\omega/2\pi = 1000$  Hz for  $\text{Pr}_2\text{CuSi}_3$  and  $\text{Nd}_2\text{CuSi}_3$ , respectively. The upward-shift of the peak position in the  $\chi'_{ac}(T)$  curve with increasing  $\omega$  could be considered as important evidence for the existence of the random spin freezing effect in  $\text{Pr}_2\text{CuSi}_3$  and  $\text{Nd}_2\text{CuSi}_3$ . However, the frequency shift rate of  $T_{ac}$  in both samples is very small. Using the expression  $\delta T_{ac} = \Delta T_{ac}/(T_{ac} \Delta \log \omega)$  (it is often used to distinguish an SG material from an SG-like system), the frequency shift rate is determined to be  $\delta T_{ac} = 0.001$  for  $\text{Pr}_2\text{CuSi}_3$  and  $\delta T_{ac} = 0.002$  for  $\text{Nd}_2\text{CuSi}_3$ . These values are roughly one order of magnitude smaller than  $\delta T_f$  (the frequency shift rate of the spin freezing temperature) reported for the cluster glass compound  $\text{Ce}_2\text{CuSi}_3$  ( $\delta T_f = 0.013$  [21]), and other typical NMAD SG systems ( $\delta T_f \sim$  several percent [4, 5, 8–11]). In addition, the  $T_f(\omega)$  data of  $\text{Ce}_2\text{CuSi}_3$  and other NMAD SG systems can be fitted to the standard expression of critical slowing down  $\tau_{\max} = \tau_0[(T_f - T_s)/T_s]^{-z\nu}$  [31], but this expression cannot describe the  $T_{ac}(\omega)$  behavior of the  $\text{Pr}_2\text{CuSi}_3$  and  $\text{Nd}_2\text{CuSi}_3$  samples. These results strongly suggest that the influence of random spin freezing in our  $\text{Pr}_2\text{CuSi}_3$  and  $\text{Nd}_2\text{CuSi}_3$  samples is very weak. Both  $\text{Pr}_2\text{CuSi}_3$  and  $\text{Nd}_2\text{CuSi}_3$  should be considered as long-range magnetic exchange interaction dominated ferromagnets with weak SG-like effect. The observed irreversible magnetism and long-time magnetic relaxation behavior seem to have their main origin in the metastable ferromagnetic ground state [28].

On the other hand, in [24] the ZFC susceptibility peak of  $\text{Nd}_2\text{CuSi}_3$  near 5 K is considered to be of antiferromagnetic origin. For our  $\text{Nd}_2\text{CuSi}_3$  sample (annealed at  $950^\circ\text{C} \times 480$  h), although the real component  $\chi'_{ac}(T)$  of the ac susceptibility shows a similar peak at  $\sim 5.6$  K (figure 4(b)) indicating a

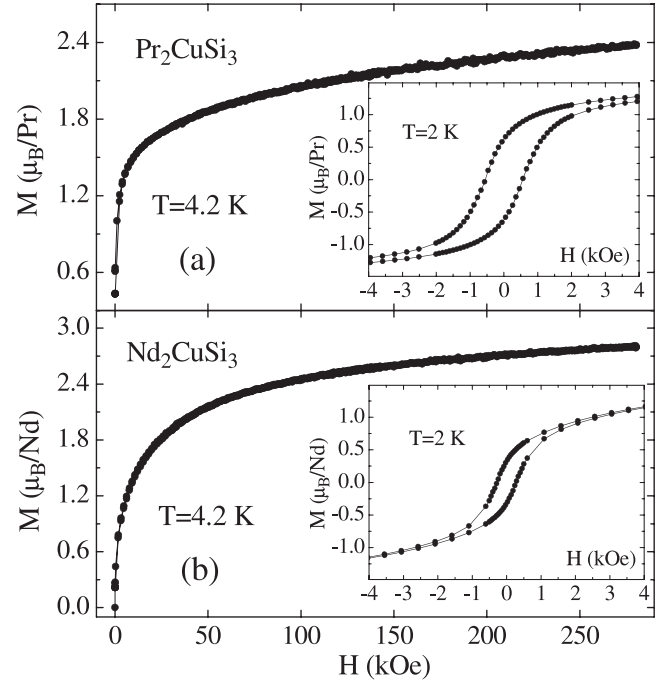


**Figure 5.** High-field magnetization  $M(H)$  up to 280 kOe for  $\text{Pr}_2\text{CuSi}_3$  (a) and  $\text{Nd}_2\text{CuSi}_3$  (b) measured at 4.2 K. The insets illustrate the low-field data of the hysteresis loops measured at 2 K using a SQUID magnetometer.

magnetic phase transition near this temperature, the imaginary component  $\chi''_{ac}(T)$ , however, shows an evident peak just below this temperature (inset of figure 4(b)) suggesting the ferromagnetic character of this phase transition as in the case of  $\text{Pr}_2\text{CuSi}_3$  (inset of figure 4(a)). In addition, the ferromagnetic features of the magnetic phase transition of  $\text{Nd}_2\text{CuSi}_3$  near 5.6 K are also manifested as a rapid increase in both  $\chi_{FC}(T)$  and  $\chi_{ZFC}(T)$  curves as  $T$  decreases near to  $T_C$  (figure 1) and the monotonic increase in the  $\chi_{FC}(T)$  curve even when the temperature is decreased down to 1.8 K (figure 2). In fact, the observation of no downturn in the  $\chi_{FC}(T)$  curves down to 1.8 K completely rules out the possibility of a simple antiferromagnetic phase transition at low temperatures [32] in both  $\text{Nd}_2\text{CuSi}_3$  and  $\text{Pr}_2\text{CuSi}_3$ . Moreover, the experimental results of high-field magnetization provide more evidence for the ferromagnetic ground state of  $\text{Pr}_2\text{CuSi}_3$  and  $\text{Nd}_2\text{CuSi}_3$ . Figures 5(a) and (b) show the  $M-H$  curves measured at 4.2 K ( $< T_C$ ) up to 280 kOe for  $\text{Pr}_2\text{CuSi}_3$  and  $\text{Nd}_2\text{CuSi}_3$ , respectively. Though complete saturation ( $M_S = 3.2 \mu_B/\text{Pr}$  for  $\text{Pr}_2\text{CuSi}_3$  and  $M_S = 3.27 \mu_B/\text{Nd}$  for  $\text{Nd}_2\text{CuSi}_3$ ) is not achieved in the field range of the measurement (may be due to the existence of magnetic anisotropy as usually observed in some ferromagnets), a sharp rise of  $M(H)$  can be observed at low fields in the magnetically ordered state and there is a tendency to attain the full moment value at high fields. With increasing  $H$ ,  $M$  reaches a value of  $2.4 \mu_B/\text{Pr}$  and  $2.8 \mu_B/\text{Nd}$  at 280 kOe and when  $H$  is returned from 280 kOe to zero a remanent magnetization of about  $0.6 \mu_B/\text{Pr}$  and  $0.3 \mu_B/\text{Nd}$  is detected for the  $\text{Pr}_2\text{CuSi}_3$  and the  $\text{Nd}_2\text{CuSi}_3$  sample, respectively. Further proof of the ferromagnetic nature can be obtained from the complete hysteresis loop measured at

2 K using a SQUID magnetometer in the field range between  $-50$  and  $50$  kOe. The low-field data are shown in the insets of figure 5 in an expanded form. As expected, one observes an open loop with remanent magnetization and coercive field of about  $0.63 \mu_B/\text{Pr}$  and  $559$  Oe for  $\text{Pr}_2\text{CuSi}_3$ , and  $0.34 \mu_B/\text{Nd}$  and  $273$  Oe for  $\text{Nd}_2\text{CuSi}_3$  at  $2$  K.

It may be of great interest to compare the magnetic properties of  $\text{Pr}_2\text{CuSi}_3$  and  $\text{Nd}_2\text{CuSi}_3$  with those reported earlier for typical SG material  $\text{U}_2\text{PdSi}_3$  [4] and ferromagnet  $\text{Nd}_2\text{PtSi}_3$  [33]. The former,  $\text{U}_2\text{PdSi}_3$ , shows the defining properties of an SG material. They are (i) the presence of a frequency dependent peak in the ac susceptibility at spin freezing temperature  $T_f$  with a relatively large  $\delta T_f$  value and the critical slowing down behavior of  $T_f(\omega)$ , and (ii) lack of periodic long-range magnetic order manifesting itself as no anomaly in either resistivity  $\rho(T)$  or specific heat  $C(T)$  curves at temperature  $T_f$ . These characteristic features cannot be observed for our  $\text{Pr}_2\text{CuSi}_3$  and  $\text{Nd}_2\text{CuSi}_3$  samples. In contrast, the  $\text{Pr}_2\text{CuSi}_3$  and  $\text{Nd}_2\text{CuSi}_3$  samples behave in a very similar manner to the metastable ferromagnetic compound  $\text{Nd}_2\text{PtSi}_3$ . In particular, the main metastable ferromagnetic characteristics displayed by  $\text{Nd}_2\text{PtSi}_3$ , e.g. (i) the rapid increase of  $\chi_{\text{FC}}(T)$  and  $\chi_{\text{ZFC}}(T)$  as  $T$  decreased near  $T_C$  followed by a sharp peak in the  $\chi_{\text{ZFC}}(T)$  curve just below  $T_C$ , and the monotonic increase in  $\chi_{\text{FC}}(T)$  below  $T_C$ , (ii) the sudden drop in the  $\rho(T)$  curve and the large peak in the  $C(T)$  curve near  $T_C$ , (iii) the sharp rise in initial magnetization  $M(H)$ , (iv) the very small  $\delta T_{\text{ac}}$  (frequency shift rate of the peak position in ac susceptibility) value, and (v) the irreversible magnetism and the long-time magnetic relaxation effect, are the same as those observed for  $\text{Pr}_2\text{CuSi}_3$  and  $\text{Nd}_2\text{CuSi}_3$  in this work. Thus it is much better to classify our  $\text{Pr}_2\text{CuSi}_3$  and  $\text{Nd}_2\text{CuSi}_3$  samples as ferromagnetically ordered materials with a very weak SG-like effect.

It has been commonly accepted that disorder and frustration are the necessary conditions of formation of an SG state. Since the electron diffraction patterns, however, indicate the ordered distribution of Cu and Si atoms in the  $\text{Pr}_2\text{CuSi}_3$  and  $\text{Nd}_2\text{CuSi}_3$  samples as stated above, a natural question to ask is why SG-like states in such magnetically ordered systems can be formed (despite its weak effect)? Although it is impossible to give a clear explanation at this stage, we can attempt to understand this behavior as follows. For an NMAD system, the disorder of nonmagnetic atoms could destroy the long-range magnetic correlation and result in the formation of finite-size granules with net magnetic moments (magnetic clusters). At low temperatures these randomly distributed clusters could interact with each other causing the formation of frustrated magnetic moments similar to what happens in amorphous or diluted metallic SG materials. In different NMAD systems, the magnetic cluster could exist with different geometric size depending on the degree of randomness and/or relative strength of magnetic interaction. For a system with completely disordered nonmagnetic atoms, the clusters could be so small that they could behave like individual spins and thus the system would show simple SG features such as the case of  $\text{U}_2\text{PdSi}_3$  with almost completely disordered Pd and Si atoms [3, 4]. With gradual increase of the orderly arranged

**Table 1.** Characteristic parameters of  $\text{Pr}_2\text{CuSi}_3$  and  $\text{Nd}_2\text{CuSi}_3$ .  $T_{\text{sf}}$ : the peak temperature in the  $C(T)$  curve;  $T_\rho$ : the kink point of the  $\rho(T)$  curve;  $T_{\text{ac}}$ : the peak temperature in the  $\chi_{\text{ZFC}}(T)$  curve at  $H = 30$  Oe;  $T_{\text{ac}}$ : the peak temperature in the  $\chi_{\text{ac}}(T)$  curve at  $\omega/2\pi = 0.1$  Hz;  $T_C$ : the defined Curie temperature, where  $d\chi_{\text{ZFC}}(T)/dT$  shows the largest value;  $\delta T_{\text{ac}}$ : the frequency shift rate of  $T_{\text{ac}}$ ;  $M_0$ : the value of magnetization at  $H = 280$  kOe and  $T = 4.2$  K;  $M_r$  and  $M_C$ : the remanent magnetization and coercive field, respectively, at  $T = 2$  K.

Compound	$T_{\text{sf}}$ (K)	$T_\rho$ (K)	$T_{\text{ZFC}}$ (K)	$T_{\text{ac}}$ (K)	$T_C$ (K)	$\delta T_{\text{ac}}$	$M_0^a$	$M_r^a$	$M_C$ (Oe)
$\text{Pr}_2\text{CuSi}_3$	8.2	9.5	9.5	9.79	9.8	0.001	2.4	0.63	559
$\text{Nd}_2\text{CuSi}_3$	5.0	4.9	5.2	5.57	5.6	0.002	2.8	0.34	273

<sup>a</sup> The unit is  $\mu_B/\text{Pr}$  for  $\text{Pr}_2\text{CuSi}_3$  and  $\mu_B/\text{Nd}$  for  $\text{Nd}_2\text{CuSi}_3$ .

atoms in the magnetic systems, the size of the magnetic cluster could become larger and larger, while the magnetic properties of the systems would change gradually from simple SG to cluster glass behaviors such as the case of  $\text{U}_2\text{RhSi}_3$  with partially disordered Rh and Si atoms [3]. Further, for a system with perfectly ordered atomic structure (such as the cases of  $\text{U}_2\text{FeSi}_3$  [7] and  $\text{U}_2\text{RuSi}_3$  [3]) or with sufficiently large magnetic clusters (such as  $\text{U}_2\text{PdGa}_3$ ,  $\text{U}_2\text{PtGa}_3$  [34], and  $\text{Nd}_2\text{PtSi}_3$  [33]) the SG effect would disappear or very weak.

Based on these analyses, the observed low-temperature ferromagnetic nature for  $\text{Pr}_2\text{CuSi}_3$  and  $\text{Nd}_2\text{CuSi}_3$  can be explained as originating from the formation of large ferromagnetic clusters in the samples below  $T_C$  due to the existence of a few randomly distributed Cu and Si atoms, while the very weak SG-like effect could be understood to result from the random exchange interactions between the clusters. Thus ferromagnetic ordering coexists with a weak SG-like effect in the investigated compounds below  $T_C$ . In addition, the disorderly arranged atoms are so small that the electron diffraction technique could not detect their presence, and sufficiently large clusters could be formed, resulting in macroscopic ferromagnetic behavior. Note that the observed irreversible magnetism, manifesting itself as the bifurcation between  $\chi_{\text{FC}}(T)$  and  $\chi_{\text{ZFC}}(T)$  curves, appears at a field dependent temperature that, in fact, is approaching  $T_C$  in a very low applied field. On the other hand, the specific heat peak appears at a temperature slightly lower than  $T_C$ . This is also a common feature among magnetic materials with cluster effect. For convenience of comparison, the peak temperature  $T_{\text{sf}}$  in  $C(T)$ ,  $T_m$  in  $\chi_{\text{ZFC}}(T)$ , and  $T_{\text{ac}}$  in  $\chi_{\text{ac}}(T)$ , the kink point  $T_\rho$  in  $\rho(T)$ , as well as some characteristic parameters of  $\text{Pr}_2\text{CuSi}_3$  and  $\text{Nd}_2\text{CuSi}_3$  are listed in table 1.

In earlier papers, we have explained the SG-like behavior observed in some other 2:1:3 NMAD compounds based on the assumption of formation of ferro- or antiferromagnetic magnetic clusters [11, 35]. A similar magnetic glass state seems to be easier to form in a magnet with relatively low magnetic moment such as in Ce or U compounds. Recently, the existence of ferromagnetic order and the cluster glass state was confirmed by Marcano *et al* in some compounds of the  $\text{CeNi}_{1-x}\text{Cu}_x$  series with even lower magnetic moment [36]. Based on small angle neutron scattering measurements, the average size of the magnetic

clusters was determined to be  $\xi = 27 \text{ \AA}$  for  $\text{CeNi}_{0.4}\text{Cu}_{0.6}$  and a much smaller value for  $\text{CeNi}_{0.8}\text{Cu}_{0.2}$  due to the highly reduced magnetic moment in this composition. Marcano *et al* explained the unusual magnetic features obtained in  $\text{CeNi}_{1-x}\text{Cu}_x$  by using a phenomenological magnetic cluster model. In their opinion, this model represents a more general situation than the particular case of  $\text{CeNi}_{1-x}\text{Cu}_x$ ; it can be used to understand the unusual magnetic properties observed in other alloyed compounds with small magnetic moments and intrinsic disorder effects [36]. Indeed, ferromagnetic or antiferromagnetic behaviors with magnetic cluster effects have also been observed in  $\text{U}_2\text{PdGa}_3$  and  $\text{U}_2\text{PtGa}_3$  ( $\xi \sim 120\text{--}150 \text{ \AA}$ ) [34],  $\text{Ce}_2\text{PdSi}_3$  ( $\xi \sim 100 \text{ \AA}$ ) [19], and many colossal magnetoresistive oxides [37–39]. Returning to the original topic, to provide the decisive evidence for the formation of ferromagnetic clusters in  $\text{Pr}_2\text{CuSi}_3$  and  $\text{Nd}_2\text{CuSi}_3$ , neutron diffraction measurements are necessary, although it is impossible for us to do this at this stage.

In conclusion, we have studied the magnetic properties of  $\text{Pr}_2\text{CuSi}_3$  and  $\text{Nd}_2\text{CuSi}_3$ , which exhibit an almost long-range magnetic order at  $T_C = 9.8$  and  $5.6 \text{ K}$ , respectively, with clear ferromagnetic characteristics near and below  $T_C$ . For both samples the dc susceptibility reveals the irreversible magnetism below  $T_C$ , while the ac susceptibility show a small shift of the peak position to high temperatures with increasing frequency, suggesting a weak SG-like effect. These characteristic features are evidently different from the results reported for typical 2:1:3 NMAD SG materials, but very similar to those found for ferromagnetic  $\text{Nd}_2\text{PtSi}_3$ . The obtained results in this work can be understood based on the magnetic cluster mechanism, and thus suggest the formation of ferromagnetic clusters in the  $\text{Pr}_2\text{CuSi}_3$  and  $\text{Nd}_2\text{CuSi}_3$  samples with very large geometric sizes probably due to the relatively highly ordered atomic arrangement.

## References

- [1] Geibel C, Kammerer C, Goring E, Moog R, Sparr G, Henseleit R, Cordier G, Horn S and Steglich F 1990 *J. Magn. Magn. Mater.* **90/91** 435
- [2] Kaczorowski D and Noel H 1993 *J. Phys.: Condens. Matter* **5** 9185
- [3] Chevalier B, Pottgen R, Darriet B, Gravereau P and Etourneau J 1996 *J. Alloys Compounds* **133** 150
- [4] Li D X, Shiokawa Y, Haga Y, Yamamoto E and Onuki Y 2002 *J. Phys. Soc. Japan* **71** 418
- [5] Li D X, Nimori S, Shiokawa Y, Haga Y, Yamamoto E and Onuki Y 2003 *Phys. Rev. B* **68** 172405
- [6] Takeda N and Ishikawa M 1998 *J. Phys. Soc. Japan* **67** 1062
- [7] Yamamura T, Li D X, Yubuta K and Shiokawa Y 2006 *J. Alloys Compounds* **408–412** 1324
- [8] Huo D, Sakurai J, Kuwai T and Ishikawa Y 2001 *Phys. Rev. B* **64** 224405
- [9] Tien C, Feng C H, Wur C S and Lu J J 2000 *Phys. Rev. B* **61** 12151
- [10] Nishioka T, Tabata Y, Taniguchi T and Miyako Y 2000 *J. Phys. Soc. Japan* **69** 1012
- [11] Li D X, Nimori S, Shiokawa Y, Tobo A, Onodera H, Haga Y, Yamamoto E and Onuki Y 2001 *Appl. Phys. Lett.* **79** 4183
- [12] Chevalier B, Lejay P, Etourneau J and Hagenmuller P 1984 *Solid State Commun.* **49** 753
- [13] Szytula A, Hofmann M, Penc B, Slaski M, Majumdar S, Sampathkumaran E V and Zygmunt A 1999 *J. Magn. Magn. Mater.* **202** 365
- [14] Majumdar S, Sampathkumaran E V, Brando M, Hemberger J and Loidl A 1999 *J. Magn. Magn. Mater.* **236** 99
- [15] Semitelou J P, Siouris J, Yakinthos J K, Schafer W and Schmitt D 1999 *J. Alloys Compounds* **283** 12
- [16] Siouris I M, Semitelou I P and Yakinthos J K 2000 *J. Alloys Compounds* **297** 26
- [17] Siouris I M, Semitelou I P, Yakinthos J K, Schafer W and Arons R R 2001 *J. Alloys Compounds* **314** 1
- [18] Li D X, Nimori S, Shiokawa Y, Haga Y, Yamamoto E and Onuki Y 2003 *Phys. Rev. B* **68** 012413
- [19] Szytula A, Hofmann M, Penc B, Slaski M, Majumdar M, Sampathkumaran E V and Zygmunt A 1999 *J. Magn. Magn. Mater.* **202** 365
- [20] Frontzek M, Kreyssing A, Doerr M, Schneidewind A, Hoffmann J-U and Loewenhaupt M 2007 *J. Phys.: Condens. Matter* **19** 145276
- [21] Hwang J S, Lin K J and Tien C 1996 *Solid State Commun.* **100** 169  
Nakamoto G, Shibai Y, Kurisu M and Andoh Y 2000 *Physica B* **281/282** 76  
Li D X, Shiokawa Y, Nimori S, Haga Y, Yamamoto E, Matsuda T D and Onuki Y 2003 *Physica B* **329–333** 506
- [22] Majumdar S, Mallik R and Sampathkumaran E V 1999 *Phys. Rev. B* **60** 6770
- [23] Tien C, Luo L and Hwang J S 1997 *Phys. Rev. B* **56** 11710
- [24] Tien C and Luo L 1998 *Solid State Commun.* **107** 295
- [25] Yubuta K, Yamamura T, Li D X and Shiokawa Y 2008 at press
- [26] Yubuta K, Yamamura T and Shiokawa Y 2006 *J. Phys.: Condens. Matter* **18** 6109
- [27] Mydosh J A 1993 *Spin Glasses: an Experimental Introduction* (London: Taylor and Francis)
- [28] Majumdar S and Sampathkumaran E V 2000 *Phys. Rev. B* **61** 43
- [29] Street R and Brown S D 1994 *J. Appl. Phys.* **76** 6386
- [30] Binder K and Young A P 1986 *Rev. Mod. Phys.* **58** 801
- [31] Hohenberg P C and Halperin B I 1977 *Rev. Mod. Phys.* **49** 435  
Gunnarsson K, Svedlindh P, Nordblad P, Lundgren L, Aruga H and Ito A 1988 *Phys. Rev. Lett.* **61** 754
- [32] Chandrasekhar Rao T V, Raj P, Mohammad Yusuf Sk, Madhav Rao L, Sathyamoorthy A and Sahni V C 1996 *Phil. Mag. B* **74** 275
- [33] Li D X, Nimori S, Shiokawa Y, Haga Y, Yamamoto E and Onuki Y 2001 *Solid State Commun.* **120** 227
- [34] Tran V H, Steglich F and Andre G 2002 *Phys. Rev. B* **65** 134401
- [35] Li D X, Yamamura T, Nimori S, Yubuta K and Shiokawa Y 2005 *Appl. Phys. Lett.* **87** 142505
- [36] Marcano N, Gomez-Sal J C, Espeso J I, De Teresa J M, Algarabel P A, Paulsen C and Iglesias J R 2007 *Phys. Rev. Lett.* **98** 166406
- [37] De Teresa J M, Algarabel P A, Ritter C, Blasco J, Ibarra M R, Morellon L, Espeso J I and Gomez-Sal J C 2005 *Phys. Rev. Lett.* **94** 207205
- [38] Burgy J, Mayr M, Martin-Mayor V, Moreo A and Dagotto E 2001 *Phys. Rev. Lett.* **87** 277202
- [39] Dagotto E 2005 *New J. Phys.* **7** 67